Progress In Electromagnetics Research C, Vol. 112, 179–192, 2021

An Improvised Non-Invasive Method with Clutter Removal for Dielectric Characterization of Terrestrial Rock Samples at S-Band Frequency

Anamiya Bhattacharya*, Deepak Putrevu, Dharmendra K. Pandey, and Arundhati Misra

Abstract—This paper presents a free-space reflection measurement technique for estimating dielectric constant and loss tangent of different materials, demonstrated for rock samples, at S-band. The method is non-contact as well as non-invasive, which is used to characterize the electromagnetic properties of different materials (in our case, rock samples) at S-band in a non-anechoic chamber environment. The technique involves the measurement of reflected signals (S_{11} data from Vector Network Analyzer) from the material under test (MUT) as well as for the surroundings. By taking the inverse-Fourier Transform of S_{11} data, the impulse-response corresponding to the reflected power from the MUT can be estimated. The proposed scheme overcomes the portability issue as well as the requirement of an anechoic environment. The measurement system consists of a single antenna (centered at 2.5 GHz), rock samples (i.e., MUT), a perfectly conducting plate, and a mounting fixture. By processing and analyzing the reflection coefficient data, the values of dielectric constant and loss tangent are calculated using the proposed algorithms which take care of clutter removal as well. The technique is validated using the estimated values of rock samples corresponding to their composition values available in the literature and found to be in good agreement. The estimation of dielectric properties of rock samples will be used to validate algorithms for science studies using SAR data of Chandrayaan-2 and other planetary missions. Hence, this measurement process will play a key role towards understanding of surface composition and features of the planetary bodies.

1. INTRODUCTION

Knowledge of dielectric properties of rock samples is an important input for geological studies. Considering the variability of rock compositions across various sites, the dielectric values available in the literature cannot be directly used in most cases. This calls for dielectric measurements of the rock samples collected from the survey site for accurate geological interpretation. The diversity in dielectric properties is observed mainly due to the composition of different minerals along with moisture content in the rock samples. At the same time, the dielectric properties of rock samples vary due to the constitution of minute grains and their compactness in the granules. The laboratory measurements of electrical properties of the earth forming rocks and minerals have played an important role [1–10] in developing electrical and electromagnetic prospecting method of mineral exploration in crystal, lunar and planetary sounding [11]. The complex dielectric responses of these materials can be represented by empirical models, in which real and imaginary dielectric responses have fractional power law dependence upon frequency. In the case of rocks and minerals, due to variation in their bulk density, chemical composition and/or crystalline structure among mineral constituents, there may be significant

Received 10 February 2021, Accepted 6 May 2021, Scheduled 10 May 2021
* Corresponding author: Anamiya Bhattacharya (anamiya2007@gmail.com).
The authors are with the Space Applications Centre (SAC), Indian Space Research Organization (ISRO), Ahmedabad, Gujarat 380015, India.

variability among measurements made for a given rock sample with spatial inhomogeneity [2–8]. The effect of microstructure on the electrical properties of the rocks and minerals of different areas in low frequency region is used to comprehend their behaviour of induced polarization [12–16].

There are a number of literatures available for free-space time domain measurement using transmission and reflection parameters in an anechoic environment. Akhtar and Akhtar in [4] use broadband absorbers and two horn antennas for simultaneous measurement of complex permittivity and thickness of dielectric samples. The operating frequency of the scheme, mentioned above, is in Ku-band, where penetration depth of the incident signal will be much less than S-band. The waveguide approach for estimating dielectric properties is also explored in [1, 3, 5]. The main disadvantage of this approach is non-retention of original shape of the sample under test (SUT) after the measurement. In [17], free-space characterization of poly-methylmethacrylate (PMMA) and poly-tetrafluroethylene (PTFE) samples has been carried out using reflection and transmission measurements, where the measurement setup is 2.1 meter high. Although the measurement is performed in the low frequency range (1–6 GHz), this setup lacks the portability, required during field study for scientific experiments. Moreover, two antennas are used for measuring transmission and reflection parameters for characterizing material properties. Non-destructive testing of a cement specimen is carried out in [18] at X-band. This measurement setup is complex, which uses a coupler, an oscillator, and an attenuation meter. In [19], complicated high-end instrumentation (internal power supply, couplers with high directivity, and powerful internal computer) is used. Therefore, the setup is very expensive and not feasible for carrying out outdoor field experiments. A detailed study of Indian rocks and minerals is also explored in [20].

During planetary exploration, the measurement of dielectric properties of the planetary surface becomes one of the prime objectives which can be derived using multi-frequency & multi-polarization Synthetic Aperture Radar (SAR) data. The estimation of these dielectric properties plays a key role in establishing its surface composition and its features. In this context, it becomes important to validate the processing methodology, prior to applying it on planetary data. With this objective in mind, an airborne L- & S-band SAR campaign has been carried out over geologically-rich region near Udaipur (Rajasthan, India), in combination with ground truth measurements of dielectric properties of the rocks found in the above regions. The dielectric characterization of the samples has been carried out using improvised noninvasive free-space measurement with clutter-removal techniques, thereby simplifying the measurement setup and making it portable for field-use as well. The objective of this paper is to describe this methodology, its theoretical basis and results.

The rest of the paper is organized as follows. In Section 2, different methods of measuring dielectric properties are illustrated, followed by the methodology adopted by us. This section also highlights the improvisations incorporated in our method. Section 3 presents the theoretical basis to derive the dielectric parameters (dielectric constant and dielectric loss) of the samples. Section 4 outlines the measurement steps which translate the theory into practice, and Section 5 discusses the measurement results and analysis. Finally, Section 6 presents the conclusions derived from the adopted methodology and the measurements carried out.

2. MEASUREMENT OF DIELECTRIC PROPERTIES

The methods of dielectric characterization may be classified broadly as invasive or destructive (e.g., waveguide method) and noninvasive or free-space (e.g., using scattering parameters, i.e., S-parameter, measurement by a network analyser). Generally, the waveguide method is used for measuring dielectric constant and dielectric loss of rock samples, crushed into powder form and placed inside the waveguide cavity. But this method suffers from some disadvantages as the samples lose their original shape. This aspect is crucial in the case of planetary rocks, which are required to be preserved for further studies and cannot be allowed to lose their original form. However, by using a free-space measurement technique, dielectric properties can be measured in a noninvasive and nondestructive way. This measurement requires the use of Vector Network Analyzer (VNA) which measures transmission and reflection coefficients with respect to frequency. The measured data can be processed further using certain computations to calculate the dielectric constant and loss tangent of the MUT.

The free space method allows measurement on the MUT irrespective of temperature and other environmental conditions; it also permits the user to operate over a wide frequency range (using an

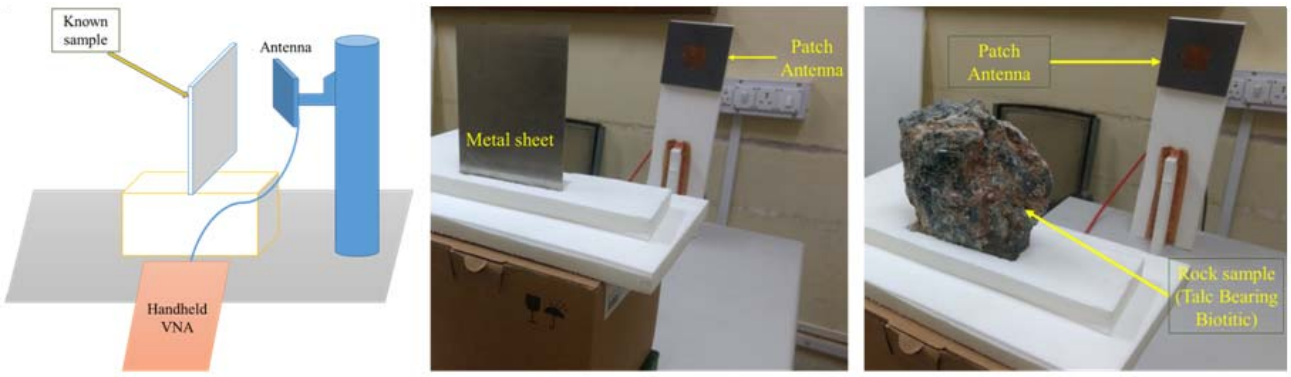

(a) (b) (c)

Figure 1. (a) Measurement set up for measuring S parameters of known samples using VNA, (b) metal sheet is kept of equivalent area corresponding to the TALC rock sample, and (c) rock (talc) sample kept in front of antenna.

antenna of corresponding frequency). However, there are certain considerations that are required to be taken care of, so that the measurements are accurate; the MUT should, typically, be flat and larger than the footprint of the antenna main-beam, and placed in the far-field of the antenna. Additionally, it should be ensured that the measurements are not contaminated by the reflections from the surroundings; this is normally taken care of by using RF absorbers for the anechoic measurement setup. Such an arrangement, however, has the disadvantage of not being portable for field (or close-to-field) measurements. The improvised measurement process adopted by us basically deals with how the above constraints are addressed. The methodology adopted by us emphasizes the noninvasive measurements based on time-domain methods in a non-anechoic environment (the measurement setup is demonstrated in Fig. 1). Such an approach revolves two-fold considerations: (i) the samples under measurement are considered to be limited and, therefore, not tampered with (which is not the case for some of the methods which call for powdering of the samples); such a methodology is mandatory for planetary return samples, and (ii) the methodology aims for a simple measurement setup, which may be portable enough to be established close to the site of ground surveys. Hence, with this framework, the measurement philosophy adopted for dielectric characterization of the rock samples addresses the above constraints as follows:

The first condition for the MUT to be flat (or smooth) can be relaxed considerably by making measurements at lower-frequency bands (S-band or lower), thereby reducing the roughness perceived by the instrumentation. The dielectric parameters so retrieved remain valid over the frequency span normally measured using radars, and hence, measurements at S-band are considered to be appropriate and are adopted for our measurement scheme.

The second condition requires MUT to be larger than the antenna main-beam footprint and placed in the far-field of the antenna. This turns out to be a conflicting requirement: the farther the MUT is from the antenna, the smaller the angular span of the antenna beam occupied by the MUT will be. Hence, to ease the requirement of placing the MUT in the far-field of the antenna, measurement with the near-ideal reference plate (a polished metal-plate) of a cross-section area same as that of the MUT is required. The measurement strategy is based on the following premise which is central to enable measurements in practical: Although the MUT is placed in the radiative near-field of the antenna with relatively lower gain than that of its far-field, a gain compensation is carried out by the reference-plate measurements at the same position. This method of compensating near-field effects is effective as the reference plate is also subjected to the lower antenna gain, same as that experienced by the MUT. However, it needs to be ensured that the MUT and reference plate are placed beyond the reactive near-field of the antenna, so that the antenna beam pattern is properly formed. This measurement scheme also ensures portability of the measurement setup and, therefore, is a cost-effective solution for measurements of dielectric properties.

An important followup to the above-mentioned measurement scenario, attempting to simplify the

setup, is that of having a single antenna configuration with normal (or near-normal) incidence of signal over the MUT. This is enabled by the measurement of S_{11} parameter using VNA. In general, this measurement corresponds to a received signal, which is the resultant of reflected signals from two sources: (i) from VNA-antenna interface port (the major component owing to return loss) and (ii) from surrounding elements including MUT, hardware jig, etc. The use of an anechoic chamber would partially address the problem by controlling the amount of contamination by external sources, but would result in a bulky setup and importantly, fall short of eliminating the VNA-antenna return loss contribution. To solve this, our measurement philosophy adopts a clutter-removal measurement process which removes the contribution of the VNA-antenna port reflections as well as those of external clutter.

In a nutshell, the highlight of the methodology adopted by us allows the measurements in a non-anechoic environment with a single antenna based S_{11} measurement, with necessary reference measurements. This requires the following three conditions to be met: (i) measurements are carried out with wide frequency span (typically $> 1\,\text{GHz}$) of the VNA, which results in improving the time-resolution (sharpening the impulse-response) obtained after inverse-Fourier Transform operation; (ii) the test bench is located such that no prominent targets are present within four times the expected time-resolution; and (iii) in addition to measurements with MUT and a polished metal-plate reference, a free-space measurement is required to be carried out with the test-fixture in the place without the MUT; using these measurements, the contribution of reflections from the antenna-VNA interface and background targets (i.e., clutter) is compensated. Use of any RF absorbers to shield the surrounding objects is not required. In short, three separate S-parameter measurements are required to be carried out corresponding to (i) free-space (i.e., set-up without MUT), (ii) a polished-metal sheet as a reference, and (iii) the MUT.

3. PRINCIPLE TO DERIVE DIELECTRIC CONSTANT AND DIELECTRIC LOSS

Permittivity is an intrinsic property of a nonconducting material which describes the ease with which a dielectric medium may be polarized; it is the proportionality constant between the electric field and electric displacement. Relative permittivity, a complex number, is a factor by which the electric field between the charges is decreased relative to vacuum and is usually denoted by ε_r. The real and imaginary components of this complex relative permittivity are known as dielectric constant and dielectric loss, respectively. Dielectric loss, represented by loss tangent or $\tan\delta$, is the measure of signal loss due to the inherent dissipation of electromagnetic energy in the substrate and is a dimensionless quantity. When the electric field is applied, polarization occurs, and charges are displaced relative to the electric field. Dielectric losses cause a reduction in the overall electric field.

The measurement principle of the complex permittivity depends on the fact that the phase and attenuation of the passing or reflecting wave vary according to the material properties, as defined above by the relative complex permittivity, ε, and expressed as

$$\varepsilon = \varepsilon_0\varepsilon_r - i\frac{\sigma}{\omega} \tag{1}$$

where $\varepsilon_0,\ \varepsilon_r,\ \sigma$, and ω represent free-space permittivity, relative dielectric constant, conductivity, and angular-frequency of signal, respectively.

The loss tangent is defined as the ratio of the imaginary component to real component of complex permittivity and can be expressed as

$$\tan\delta = \frac{\sigma}{\omega\varepsilon_0\varepsilon_r} \tag{2}$$

For measuring the dielectric constant of different rock samples, the following is the formulations relating the electric field intensities and power measurement, as they take place at different interfaces [3, 4]:

If E_{incident} is the electric field of the wave incident at the MUT interface and Γ_0 the voltage reflection coefficient of the MUT, then the electric field of the reflected wave can be given by

$$E_{\text{measured}} = \Gamma_0 E_{\text{incident}} + \sum_{i=1}^{N} E_i \tag{3}$$

where the summation of E_i represents the clutter, owing to the objects surrounding the target being tested. The power corresponding to this can be derived using Poynting relationship, as given below:

$P_{\text{avg}} = \frac{E_0}{2|\eta|}e^{-2\alpha z}$, where η and α are the intrinsic impedance and attenuation of the medium, with a thickness, z. Here, E_0 represents the peak of the electric field in consideration. Under free-space conditions, $\alpha = 0$, and η is uniformly applicable at any interface point. Hence, without loss of generality, reflected power measured by VNA, P_{measured}, can be represented as:

$$P_{\text{measured}} = E^2_{\text{measured}} = \left[\Gamma_0 E_{\text{incident}} + \sum_{i=1}^{N} E_i\right]^2 \tag{4}$$

$$P_{\text{measured}} = \Gamma_0^2 E^2_{\text{incident}} + \sum_{i=1}^{N} E_i^2 + \sum_{i,j=1,i\neq j}^{N} E_i E_j \tag{5}$$

As the reflections from surrounding objects will be uncorrelated $\sum_{i,j=1,i\neq j}^{N} E_i E_j = 0$,

$$P_{\text{measured}} = \Gamma_0^2 E^2_{\text{incident}} + \sum_{i=1}^{N} E_i^2 \tag{6}$$

Hence, considering $P_{\text{incident}} = E^2_{\text{incident}}$ and $P_{\text{clutter}} = \sum_{i=1}^{N} E_i^2$, P_{measured} can be given as:

$$P_{\text{measured}} = \Gamma_0^2 P_{\text{incident}} + P_{\text{clutter}} \tag{7}$$

The formulations for different cases of dielectric constant and loss estimation will be based on power relationship as derived above in Eq. (7). The following is the specific cases.

3.1. For Case I Corresponding to Metal Plate (Reference) Measurement, Shown in Fig. 2

Let the power incident on metal plate (reference) be P_{incident}. As the wave is incident normally on the polished metal surface (considered to have a reflection coefficient close to unity), almost full reflection of the power can be considered. Therefore, power reflected, $P_{\text{reflected}}$, from the metal surface can be written as: $P_{\text{reflected}} \approx P_{\text{incident}}$. However due to the presence of clutter owing to other scatterers surrounding the fixture/setup, the power received by the measurement system, P_{measured}, can be given as:

$P_{\text{measured}} = P_{\text{reflected}} + P_{\text{clutter}}$ represents power measured for metal reference as P_{ref}, and we now have:

$$P_{\text{reflected}} = P_{\text{incident}} + P_{\text{clutter}} \tag{8}$$

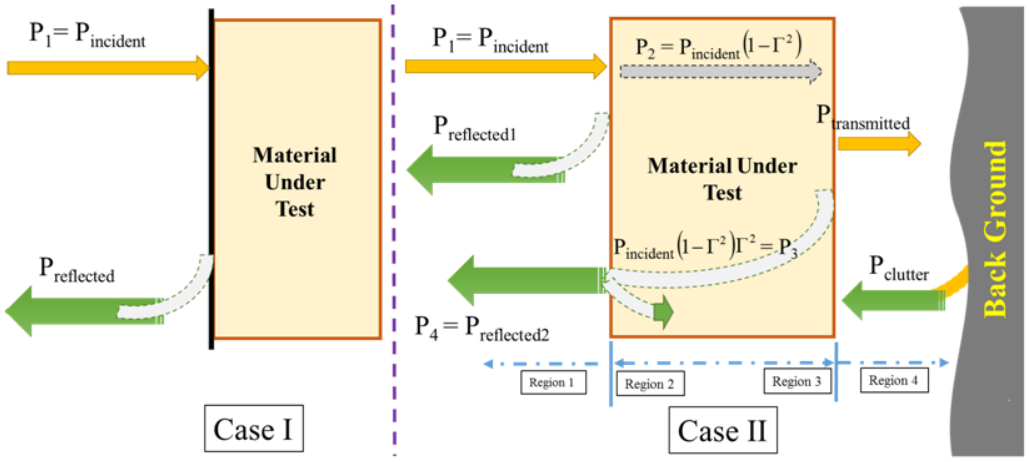

Figure 2. Electromagnetic wave flow diagram for different cases; (Case I) Incident wave on metal surface(represented as a thick solid line) kept in front of MUT, (Case II) incident wave on MUT (rock sample).

3.2. For Case II as Shown in Fig. 2

The wave is incident normally on MUT possessing an unknown voltage reflection coefficient Γ. The power reflected, $P_{\text{reflected1}}$, corresponds to:

$$P_{\text{reflected1}} = \Gamma^2 P_{\text{incident}} \tag{9}$$

This results in part of the incident power being transmitted and the rest being reflected back. With this consideration, the transmitted power (within MUT) can now be represented as:

$$P_2 = P_{\text{incident}}(1 - \Gamma^2) \tag{10}$$

This power is likely to suffer two more reflections inside the MUT, at the interfaces marked as "region-3" and "region-2", before emerging in the direction of measurement, which can be given as:

$$P_{\text{reflected2}} = P_{\text{incident}}(1 - \Gamma^2)\Gamma^2(1 - \Gamma^2) \tag{11}$$

This power, $P_{\text{refllected2}}$, owing to multiple reflections is negligible compared to that from the first interface reflection, $P_{\text{refllected1}}$. Hence, the net power measured, P_{MUT}, is given by:

$$P_{\text{MUT}} = \Gamma^2 P_{\text{incident}} + P_{\text{clutter}} \tag{12}$$

3.3. For Case II as Shown in Fig. 3

This measurement is meant for dielectric loss estimation and requires a metal reference plate to be kept behind the MUT, with minimum possible air-gap, as shown in Fig. 3. As mentioned in the previous case, there is a fraction of the incident power, given by $P_{\text{incident}}(1 - \Gamma^2)$ which will propagate through the MUT, to be reflected back at the interface of MUT-metal reference, thereby traversing the MUT twice its thickness, d, resulting in power reduction by a factor of $e^{-4\alpha d}$ where α represents the attenuation constant of the MUT. Another reflection at the MUT-air results in the residual power of $P_{\text{incident}}(1-\Gamma^2)^2 e^{-4\alpha d}$ which emerges from the MUT towards the antenna of measurement system. The net power measured will be:

$$P_{\text{MUT, LOSS}} = P_{\text{incident}}(1 - \Gamma^2)^2 e^{-4\alpha d} + P_{\text{clutter}} \tag{13}$$

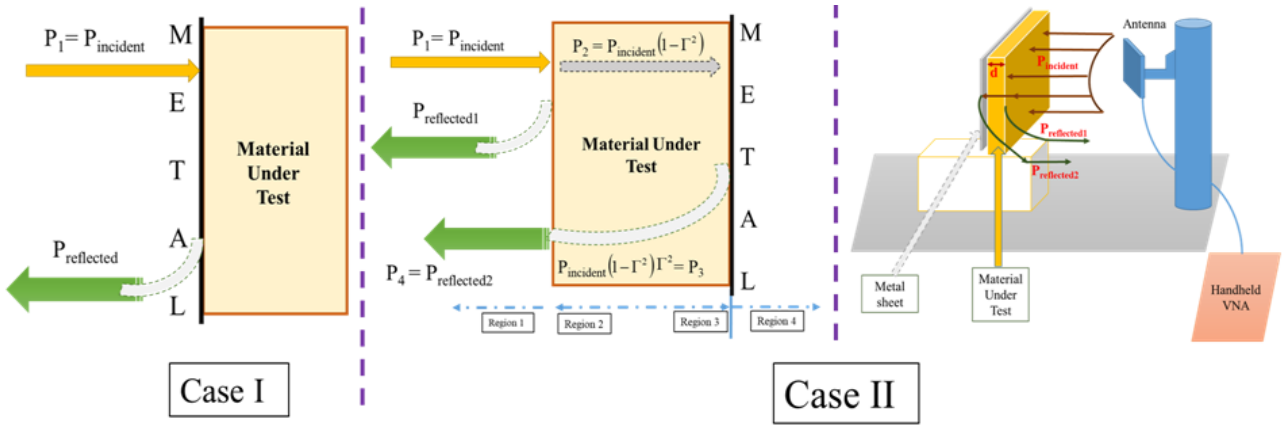

Figure 3. Measurement system configuration for measuring dielectric loss; (Case I) Incident wave on metal surface (represented as a thick solid line) kept in front of MUT, (Case II) incident wave on MUT, with metal plate (shown with a thick solid line) kept behind the MUT.

3.4. For Clutter Measurements (With Only Elements Surrounding the MUT Fixture)

The reflection from clutter is measured without MUT but keeping rest of the surrounding objects undisturbed from the previous two measurements. This is represented by the quantity P_{clutter}.

From P_{clutter} measured in this step, P_{MUT} and P_{ref} from Eq. (8) and Eq. (12), reflection coefficient Γ can be derived:

$$\Gamma = \sqrt{\frac{P_{\text{MUT}} - P_{\text{clutter}}}{P_{\text{ref}} - P_{\text{clutter}}}} \tag{14}$$

3.5. Dielectric Constant Estimation from the Above Measurements

Consider η, ε, and μ as characteristic impedance, permittivity, and permeability, respectively, of two interfacing media represented by subscripts 1 & 2.

$$\Gamma = \frac{\eta_2 - \eta_1}{\eta_2 + \eta_1}$$

$$\Gamma = \frac{\sqrt{\dfrac{\mu_2}{\varepsilon_2}} - \sqrt{\dfrac{\mu_1}{\varepsilon_1}}}{\sqrt{\dfrac{\mu_2}{\varepsilon_2}} + \sqrt{\dfrac{\mu_1}{\varepsilon_1}}} = \frac{\sqrt{\varepsilon_1} - \sqrt{\varepsilon_2}}{\sqrt{\varepsilon_1} + \sqrt{\varepsilon_2}},$$

with $\varepsilon_1 = \varepsilon_2 = \varepsilon_r$ and $\mu_1 = \mu_2 = \mu$ for typical dielectric material $\Gamma = \frac{\sqrt{\varepsilon_r}-1}{\sqrt{\varepsilon_r}+1}$. Therefore,

$$\varepsilon_r = \left(\frac{1+\Gamma}{1-\Gamma}\right)^2 \tag{15}$$

3.6. Dielectric Loss Estimation from the Above Measurements

From the estimated values of reflection coefficient (Γ), measured values of MUT thickness, d, and power measurements, $P_{\text{MUT, LOSS}}$, P_{MUT}, and P_{clutter}, we can derive the attenuation constant of MUT given by α (using Eqs. (12) to (13)), using the following relation:

$$e^{-4\alpha d} = \frac{P_{\text{MUT, LOSS}} - P_{\text{clutter}}}{P_{\text{incident}}(1-\Gamma^2)^2} = \frac{P_{\text{MUT, LOSS}} - P_{\text{clutter}}}{\dfrac{P_{\text{MUT}} - P_{\text{clutter}}}{\Gamma^2}(1-\Gamma^2)^2} \tag{16}$$

From attenuation constant α, conductivity (σ) can be estimated by using

$$\sigma = \frac{2\alpha\sqrt{\varepsilon_r}}{\eta_0} \tag{17}$$

where η_0 and ε_r are the free space intrinsic impedance and dielectric constant. From Eq. (17), loss tangent ($\tan\delta$) can be estimated using Eq. (2).

4. MEASUREMENT PROCESS

As discussed in Section 1 of this paper, our requirement of dielectric characterization of rock samples was necessitated as inputs for validation of SAR data based algorithm for the retrieval of dielectric parameters. The rock samples for this purpose have been collected through ground surveys over geologically-rich regions near Udaipur (Rajasthan, India) covered during airborne SAR campaign.

The rock samples collected include dolomite, marble, quartz, micaceous phyllite, quartzite, and slate. The dielectric measurements of these samples have been based on the theoretical treatment and dealt with in the previous section. It is important to note that this measurement process is generic in nature, as it is applicable to all samples in consolidated form. However, there may be slight differences in fixture setup based on the dimensions of the samples.

In our case, measurements were carried out in S-band frequency (2.5 GHz), using a patch antenna fixed at one end of the fixture. Before starting the measurements, handheld VNA (Keysight Technologies Vector Netwwork Analyzer N9918A) is connected with low-loss cables and calibrated for open, short, matched-load, and through-ports, for the frequency range of operation, i.e., 1 to 4 GHz. The calibration is done at the ends of the cables meant for connecting the antenna. As already discussed earlier, four

measurements are required to be made for one set of dielectric characterization, corresponding to (i) the background, (ii) reference metal plate, (iii) MUT alone, and (iv) MUT with metal plate behind it. Measurements (i) to (iii) will be used to derive dielectric constant and measurements (i) to (iv) for dielectric loss. It is important to ensure that the background remains the same, i.e., position and orientation of the objects remain undisturbed during the full-set of (i) to (iv) measurements.

The measurement fixture is set up with the sample holder aligned with the antenna and kept at an appropriate distance from it, as shown in Fig. 1. It has to be ensured that the spacing between the antenna and the MUT is more than thrice the wavelength, i.e., beyond reactive near-field. For our frequency of operation (2.5 GHz), this minimum spacing comes out to be 36 cm. With an additional margin, we have considered a spacing of 60 cm, i.e., five times the wavelength.

The measurement with an empty sample holder is referred to as "background measurement" and is used for clutter removal from those of the rest. This is followed by measurements for a flat polished metal plate for reference and that of MUT, itself. The reference flat-plate and the MUT are then placed (as shown in Figs. 1(b) & 1(c), respectively), one after the other, on the sample holder, and the S-parameter measurement is performed again. An inverse-FFT on the S_{11} data will result in an impulse-response corresponding to the reflected power from the background, MUT, or the reference plate, as the case may be. The processed data can be corrected for return loss component at VNA-antenna interface and the clutter by subtracting time-domain response of free-space measurement from those of MUT (Fig. 1(c)) and reference plate. The position of the peak from the response will correspond to the distance between the antenna and the dominant scattering object (e.g., MUT or flat-plate). The dielectric properties can be determined by processing the measured reflection coefficient (S_{11}) data of MUT with respect to that of reference plate.

Prior to reference plate measurement, the projected cross section of the rock sample is used to determine the area of the reference plate. As different MUTs have different cross-section areas, a dedicated reference plate (fabricated and polished) is used for each MUT. The location of the metal-reference is kept the same as that of the MUT surface being measured. As the thicknesses of the MUT and reference plate are different, the diffraction effects for each will also be different causing some inaccuracy in compensation factor, while deriving the net impulse response contribution.

For calculating the dielectric constant and loss tangent, the measurement process is elaborated stepwise as follows:

Step 1: First calibrate the VNA for a particular frequency range (1 GHz to 4 GHz). Sweep: A sufficiently high number; 10001 samples, in our case.

Step 2: In trace selection, take S_{11} complex data. All S_{11} measurements in the following steps involve a frequency sweep over 1 GHz to 4 GHz, with the above number of samples.

Step 3: Place the metal sheet of equivalent area corresponding to the sample and measure required S-parameter (S_{11}). The position of the metal sheet should be beyond the reactive near-field of the antenna.

Step 4: The metal-sheet can now be replaced with the MUT for the S_{11} measurement, while ensuring that the position is not disturbed, and lateral profile of antenna illumination remains the same for reference metal sheet (in the previous step) and the MUT. Measure the S_{11}.

Step 5 (Required only for loss-measurements): Place the metal sheet closely behind the MUT such that any gap between the two is minimum, and measure S_{11} parameter. Here, it is important to note that the reflected signal passes through the MUT twice, which is considered in the formulations to derive the dielectric loss, described in Section 3.

Step 6: Remove the MUT and measure the free space S_{11}.

Step 7: Each measurement data (real & imaginary components of S_{11}) is initially in the frequency domain corresponding to the centre-frequency and the span selected. An inverse-FFT (IFFT) operation is done to bring the same into the time-domain (A MATLAB [21] based program is used in this respect). The output is basically a compressed time-domain response (termed as impulse-response). A symmetrical zero-padding operation prior to IFFT affects an interpolation operation and smooths the impulse-response. The frequency span and zero-padding settings have to be kept the same for all three measurements corresponding to: MUT, free-space, and metal-reference.

Step 8: Each time domain response (complex) of sample and metal sheet is compensated for free space. The compensated response peaks at a time corresponding to the round-trip time between

antenna and MUT.

Step 9: Using the impulse-responses, determine the peak-powers for MUT sample and reference metal sheet, and take their ratio to get the reflection coefficient (Γ). Using this, the dielectric constant (real component of the complex dielectric permittivity) of the MUT can be calculated from Eq. (15).

Step 10: From Eq. (16) and Eq. (17), attenuation coefficient, conductivity, and thereby, loss tangent ($\tan\delta$, Eq. (2)) can be estimated.

5. ANALYSIS AND MEASURED RESULTS

Based on the theoretical treatment given in Section 3 and the measurement process outlined in Section 4, the S-parameter measurements have been carried out over the rock-samples (as shown in the inset of Figs. 4(a) to 4(f)), collected from the Udaipur region. Prior to the start of the measurements of the rock samples, glass material of known dielectric constant (of 5.3) was measured. The dielectric constant for glass material was calculated to be 5.28 based on the above method, which is closely matched to the expected value. The glass material was used to help the calibration of the setup; i.e., the placing of MUT, distance between probes, and placement of MUT at a particular height.

Subsequent to calibration using glass sample, the measurements have been performed for various samples (marble, talc, quartz, dolomite, quartzite, schist). The S_{11} measurements (with a frequency sweep from 1 to 4 GHz in 10001 steps) is interpolated by a factor of 3 by zero-padding with 10000 samples on either side, before taking the inverse-FFT. The resulting time-domain response will be dominated by the antenna-port reflection component, which is present in all the measurements for MUT, metal, and clutter. It is only after clutter compensation that the antenna-port reflection component is eliminated, and the variability due to MUT or metal can be observed, as shown in Fig. 4. It is for this reason that the plots prior to the above compensation are not presented. The peak values indicated in Figs. 4(a) to 4(f) are used to calculate the reflection coefficient and thereafter the dielectric constant of the MUT, as presented in Table 1. It has been found that the measured results match closely with the literature

Table 1. Summary of dielectric constant for different samples.

Sample name	Reflection coefficient	Dielectric constant (theoretical, as per presence of dominant minerals)	Dielectric constant (real)
Marble	0.254	2.5–7	2.82
Talc	0.252	Near to 3	2.8
Quartz	0.236	Near to 3	2.61
Dolomite	0.486	7.7–8.5	8.35
Quartzite (L-7/2)	0.396	5.2–5.7	5.34
Schist (L-4)	0.513	8.9–10	9.65

Table 2. Summary of dielectric loss and conductivity for different samples.

Sample name	Only MUT (Amplitude: A1)	Metal Back side (Amplitude: A2)	Ratio (in Power) $(A2/A1)^2$	Thickness (meter)	Attenuation constant (α) Nepers/meter	Conductivity (σ) Siemens/meter	Loss Tangent
Marble	0.002031	0.002172	1.143668	0.037	16.71094	0.366	0.466
Talc	0.002454	0.002556	1.084857	0.050	12.71992	0.301	0.386
Quartz	0.001906	0.003645	3.657205	0.062	5.953764	0.058	0.079
Dolomite	0.003941	0.002408	0.373336	0.030	15.74568	0.331	0.143
Quartzite (L-7/2)	0.003118	0.002688	0.743201	0.057	7.931275	0.117	0.079
Schist (L-4)	0.004574	0.003706	0.656475	0.018	15.90327	0.336	0.125

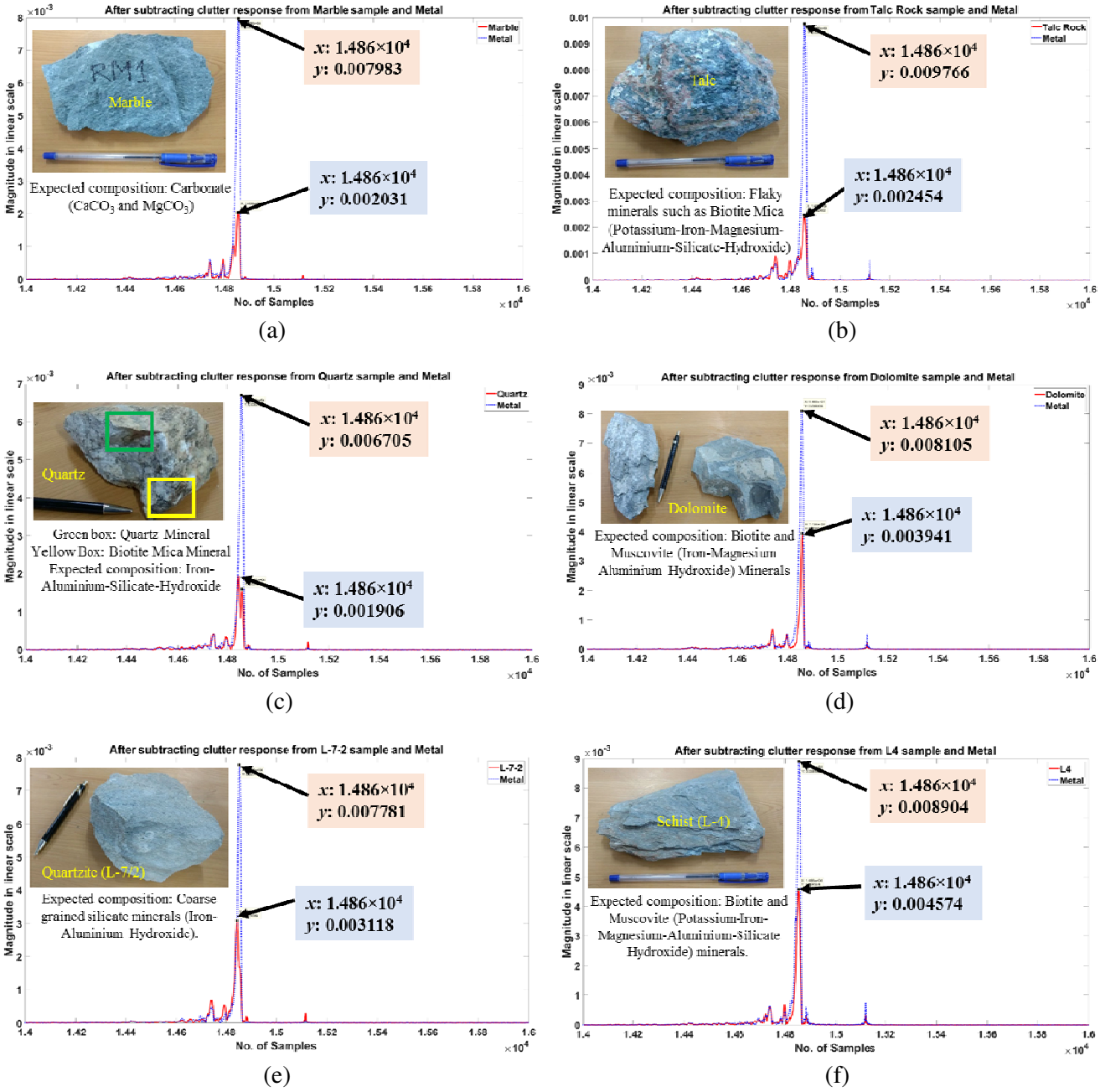

Figure 4. Time domain response after clutter power compensation, for each pair of cases of metal reference and MUT represented by blue and red curves, respectively. The peak values shown are used to derive the dielectric constant. Photograph of the rock sample is shown as an inset in each graph. (a) MUT: marble rock sample. (b) MUT: talc rock sample. (c) MUT: quartz rock sample. (d) MUT: dolomite rock sample. (e) MUT: quartzite (L-7/2) rock sample. (f) MUT: Schist (L-4) rock sample.

data of rock samples. Similarly, results illustrated in Figs. 5(a) to 5(f) correspond to the case of a metal-reference placed behind the rock sample, for dielectric loss (in terms of loss tangent) estimation. These measurements along with derived dielectric constant values are used (as described in Sections 3 & 4) to quantify the loss tangent of the MUT.

Dielectric constant and loss tangent for rock samples are estimated, and the values are found varying in the range of 2.8 to 9.6 (Table 1) and 0.08 to 0.47 (Table 2) respectively depending upon the

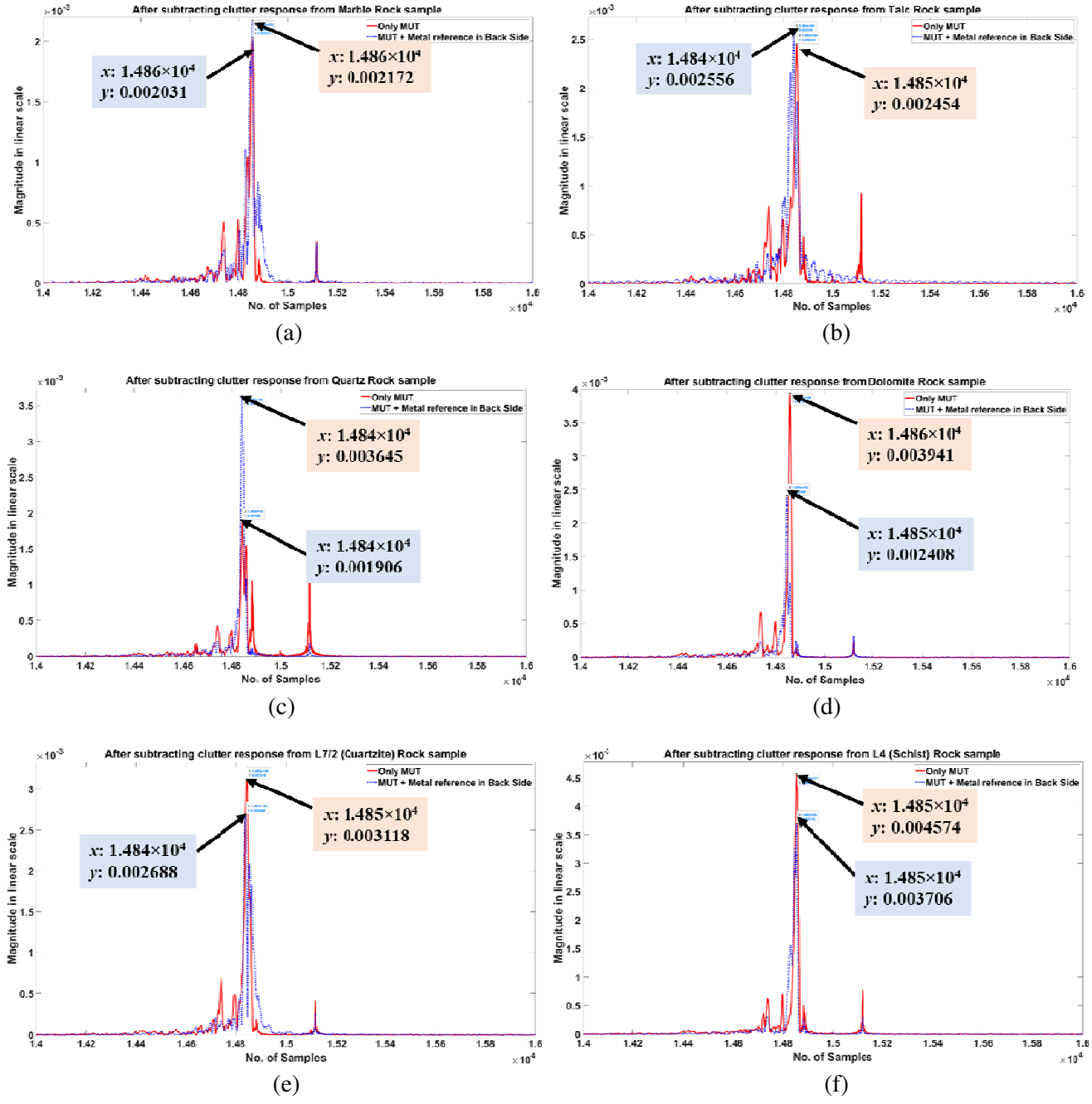

Figure 5. Time domain response after clutter power compensation, for each pair of cases of MUT alone and metal reference kept behind MUT, represented by red and blue curves, respectively. The peak values shown are used to derive the dielectric loss. (a) MUT: marble rock sample. (b) MUT: talc rock sample. (c) MUT: quartz rock sample. (d) MUT: dolomite rock sample. (e) MUT: quartzite (L-7/2) rock sample. (f) MUT: Schist (L-4) rock sample.

composition of minerals, packing density, and thickness of rock samples.

Table 1 refers to the dielectric constant estimation from which we can classify marble, talc, and quartz samples as low dielectric constant ones, whereas, dolomite, quartzite, and schist are of relatively higher values. Table 2 illustrates the dielectric loss estimation, along with intermediate values obtained during the process.

The combined effect of dielectric constant and loss leads to interesting observation of the power ratio mentioned in Table 2. This value represents the ratio of reflected power corresponding to metal reference placed behind MUT and that of only the MUT, respectively; the ratio is higher than unity for some and lower for some. To understand the it, let us consider the following: When the dielectric constant of MUT is low (e.g., marble, talc, and quartz), the first reflection from MUT is less than that for the case "metal placed behind MUT".

This results in higher ratio (> 1) for these samples. Out of these three rock samples, with similar dielectric constant values, the ratio for quartz is found to be relatively higher, which is explainable when the MUT loss is less (resulting in more signal at the MUT-metal interface and correspondingly higher signal returning to the antenna). This is consistent with the corresponding values of derived loss tangents.

The above explanation also holds well for the other three materials, viz, dolomite, quartzite (L-7/1), and schist (L-4). Their higher dielectric constant values result in higher backscatter from the first MUT interface itself, which results in lower value of the ratio (< 1). Out of these three, the quartzite sample (L-7/2) has a relatively higher ratio, consistent with the estimated value of lower loss-tangent.

6. CONCLUSIONS

This paper presents the methodology of measuring dielectric constant and dielectric loss of an unknown sample in a noninvasive way using free-space methods. The presented method has the following key characteristics:

(a) the method is noninvasive in order to keep the rock samples intact for further studies. This is particularly crucial in the case of planetary samples.

(b) the measurement considers the MUT in radiative near-field of the antenna, which enables a practical measurement scenario while easing the far-field measurement constraints. The MUT as well as the reference plate (of same cross-section as the MUT) experiences the same amount of lower antenna gain, owing to their placement in radiative near-field. Such an arrangement enables gain-independent reflection measurements.

(c) Measurement is based on monostatic (single-antenna) configuration with S_{11} parameter of VNA, to enable normal (or near-normal) incidence of signal over MUT or reference plate, thereby reducing errors due to nonuniform scattering effects.

(d) Major error component of VNA-antenna port reflection in S_{11} measurement is nullified in the process of clutter compensation using free-space measurements. Background contamination is taken care of without any requirement for RF absorbers. This makes the setup simple and portable enough to be used in outdoor field conditions as well.

The results of the measurements presented in Section 5 show a good retrieval accuracy and thereby, illustrate the efficacy of the measurement methodology. As a future work, further improvement of retrieval accuracy may be attempted using data preprocessing techniques, like, fuzzy, neuro-fuzzy, artificial neural network (ANN) technique, genetic algorithm (GA) as described in [22–24].

ACKNOWLEDGMENT

The authors are thankful to the Director, SAC for his constant encouragement and the SAC teams of Antenna Systems and Mechanical fabrication for their immense support during the above work. The authors are also thankful to Shri Tathagata Chakraborty, Geologist at SAC, responsible for ground-truth rock samples collection and his valuable insights regarding the samples under study. The authors also acknowledge the reviewers for their insightful comments which have added great value to the paper.

REFERENCES

1. Prakash, A., J. K. Vaid, and A. Mansingh, "Measurement of dielectric parameters at microwave frequencies by cavity perturbation technique," *IEEE Transactions on Microwave Theory and Techniques*, Vol. 27, No. 9, 791–795, Sep. 1979.

2. Orlob, C., T. Reinecke, E. Denicke, B. Geck, and I. Rolfes, "Compact unfocused antenna setup for X-band free-space dielectric measurements based on line-network calibration method," *IEEE Transactions on Instruments and Measurement*, Vol. 62, No. 7, 1982–1989, Jul. 2013.
3. Jha, A. and M. J. Akhtar, "A generalized rectangular cavity approach for determination of complex permittivity of materials," *IEEE Transactions on Instruments and Measurement*, Vol. 63, No. 11, 2632–2641, Nov. 2014.
4. Akhtar, Z. and M. J. Akhtar, "Free-space time domain position insensitive technique for simultaneous measurement of complex permittivity and thickness of lossy dielectric," *IEEE Transactions on Instruments and Measurement*, Vol. 65, No. 10, 2394–2405, Oct. 2016.
5. Webb, W. E. and R. H. Church, "Measurement of dielectric properties of minerals at microwave frequencies," Report by United States, Department of the Interior, 1986.
6. Akhtar, M. J., L. Feher, and M. Thumm, "Measurement of dielectric constant and loss tangent of epoxy resins using a waveguide approach," *IEEE International Symposium on Antennas and Propagation Society*, 3179–3182, 2006.
7. Kumar, S. B., U. Raveendranath, P. Mohanan, K. T. Mathew, M. Hajian, and L. P. Ligthart, "A simple free-space method for measuring the complex permittivity of single and compound dielectric materials," *Microwave and Optical Technology Letters*, Vol. 26, No. 2, 117–119, Jul. 2000.
8. Ghodgaonkar, D. K., V. V. Varadan, and V. K. Varadan, "A free-space method for measurement of dielectric constants and loss tangents at microwave frequencies," *IEEE Transactions on Instruments and Measurement*, Vol. 37, No. 3, 789–793, Jun. 1989.
9. Skocik, P. and P. Neumann, "Measurement of complex permittivity in free-space," *25th DAAAM International Symposium on Intelligent Manufacturing and Automation*, 100–104, 2014.
10. Courtney, C. C., "Time-domain measurement of the electromagnetic properties of materials," *IEEE Transactions on Microwave Theory and Techniques*, Vol. 46, No. 5, 517–522, May 1998.
11. Singh, R. P., M. P. Singh, and T. Lal, "Laboratory measurement of dielectric constant and loss tangent of Indian rock samples," *Annals of Geophysics*, 121–140, Jun. 1980.
12. Bapna, P. C. and S. Joshi, "Measurement of dielectric properties of various marble stones of Mewar region of Rajasthan at X-band microwave frequencies," *International Journal of Engineering and Innovative Technology*, Vol. 2, 180–186, Jan. 2013.
13. Gupta, S. L., Z. Akhtar, M. Bhaskar, and M. J. Akhtar, "A novel half space time-domain measurement technique for one dimensional microwave imaging," *IEEE ARFTG Conference*, 2014.
14. Gupta, S. L., Z. Akhtar, M. Bhaskar, and M. J. Akhtar, "Qualitative analysis of moisture content in cement based material using microwave non-destructive testing," *IEEE APS Conference*, 924–925, 2014.
15. Hasar, U. C., "Unique permittivity determination of low-loss dielectric materials from transmission measurements at microwave frequencies," *Progress In Electromagnetics Research*, Vol. 107, 31–46, 2010.
16. Barman, B., Z. Akhtar, and M. J. Akhtar, "Microwave testing of cement based material," *International Microwave and RF Conference*, Dec. 14–16, 2013.
17. Goncalves, F. J. F., A. G. M. Pinto, R. C. Mesquita, E. J. Silva, and A. Brancaccio, "Free-space material characterization by reflection and transmission measurements using frequency-by-frequency and multi-frequency algorithms," *Electronics*, Vol. 7, 260, 2018.
18. Hasar, U. C., "Non-destructive testing of hardened cement specimens at microwave frequencies using a simple free-space method," *NDT & E International Journal*, 550–557, Elsevier, 2009.
19. Lasri, T., D. Glay, L. Achrait, A. Mamoni, and Y. Leriy, "Microwave methods and systems for nondestructive control," *Subsurface Sensing Technol. Appl.*, 141–160, 2000.
20. Singh, J. and P. K. Singh, "Studies of the dielectric constant of Indian rocks and minerals and some other materials," *Pure and Applied Geophysics*, Vol. 135, No. 4, 601–610, Jan. 1991.
21. www.mathworks.com/products.matlab/html.

22. Mohammed, M., A. Sharafati, N. Al-Ansari, and Z. M. Yaseen, "Shallow foundation settlement quantification: Application of hybridized adaptive neuro-fuzzy inference system model," *Advances in Civil Engineering*, article ID 7381617, 2020.
23. Postorino, M. N. and M. Versaci, "A geometric fuzzy-based approach for airport clustering," *Advances in Fuzzy Systems*, article ID 201243, 2014.
24. Zubaidi, S. L., H. Al-Bugharbee, S. O. Martorell, S. K. Gharghan, I. Olier, K. S. Hashim, N. S. S. Al-Bdairi, and P. Kot, "A novel methodology for prediction urban water demand by wavelet denoising and adaptive neuro-fuzzy inference system approach," *Water Journal*, Vol. 12, No. 6, 1628, 2020.